

Precise calculation for heavy gauge boson production in the LHT model

Guo Lei, Zhang Ren-You and Ma Wen-Gan

Department of Modern Physics, University of Science and Technology of China (USTC),
Hefei, Anhui 230026, P.R.China

E-mail: guolei@mail.ustc.edu.cn, zhangry@ustc.edu.cn, mawg@ustc.edu.cn

Abstract. In the framework of the littlest Higgs model with T parity, we study the W_H/Z_H+q^- and W_H -pair productions at the CERN Large Hadron Collider up to the QCD next-to-leading order (NLO). The kinematic distributions of final decay products and the theoretical dependence of the cross section on the factorization/renormalization scale are analyzed. We adopt the PROSPINO scheme in the QCD NLO calculations to avoid double counting and keep the convergence of the perturbative QCD description. By using the subtraction scheme, the QCD NLO corrections enhance the leading order cross section with a K-factor in the range of $1.00 \sim 1.43$ for $W_H(Z_H)q^-$ production process, and in the range of $1.09 \sim 1.22$ for the W_H pair production process.

1. Introduction

Although the standard model (SM) [1, 2] provides a remarkably successful description of high energy physics phenomena at the energy scale up to 100 GeV , it leaves a number of theoretical problems unsolved. Many extended models are proposed to deal with these problems such as grand unified theories [3], supersymmetric models [4], extra dimensions models [5], left-right symmetric models [6], B-L (baryon number minus lepton number) extended SM models [7], little Higgs models [8] and many more. Each of these models has motivation to solve one or more of the problems that the SM encounters. Among them the little Higgs models deserve attention due to their elegant solution to hierarchy problem and are proposed as one kind of electroweak symmetry breaking (EWSB) models without fine-tuning in which the Higgs boson is naturally light as a result of nonlinearly realized symmetry [9]-[14]. The littlest Higgs (LH) model [15], an $SU(5)/SO(5)$ nonlinear sigma model [11], is the most simplest version of little Higgs models, in which a set of new heavy gauge bosons (A_H, W_H, Z_H) and a vector-like quark (T) are introduced to cancel the quadratic divergence contribution to Higgs boson mass from the SM gauge boson loops and the top quark loop respectively. However, this model predicts large corrections to electroweak precision observables and the scale of the global symmetry breaking f , is constrained by experimental data [12], which set severe constraints on the new heavy particle masses and the model parameters. For instance, recent experimental measurements on the decay processes of $W_H^\mp \rightarrow l^\mp \bar{\nu}^{(-)}$ and $Z_H \rightarrow l^+l^-$ provide the constraints of $M_{W_H} > 2.18 \text{ TeV}$ and $M_{Z_H} > 1.83 \text{ TeV}$ [16, 17]. These constraints would enforce the symmetry breaking scale f , which characterizes the mass of new particles, to be larger than 2.5 TeV and 3 TeV respectively.

Consequently, the cutoff scale $\Lambda \sim 4\pi f$ becomes so large that calls for the fine-tuning between the electroweak scale and the cutoff scale again.

By introducing a discrete symmetry, the T parity, the littlest Higgs model with T parity (LHT) [18]-[22] offers a viable solution to the naturalness problem of the SM, and also predicts a set of new heavy fermions, gauge bosons as well as a candidate for dark matter. In the LHT, all the SM particles are T -even and almost all the new heavy particles are T -odd. Due to the different T parity quantum numbers, the SM gauge bosons cannot mix with the new gauge bosons in the LHT. This would alleviate the constraints from the electroweak precision tests and thus allows the scale f to be significantly lower than 1 TeV [21]. For instance, due to the T parity conservation, the processes $W_H^\mp \rightarrow l^\mp \bar{\nu}^{(-)}$ and $Z_H \rightarrow l^+l^-$ are forbidden, and the only decay modes of these T -odd heavy gauge bosons are $W_H \rightarrow A_H W$ and $Z_H \rightarrow A_H H$. In this case, the leptons are produced from the decays of W and H , but not from the heavy gauge bosons directly. Therefore, these T -even gauge bosons escape from the experimental constraints shown in Refs.[16, 17]. Furthermore, as a lightest T -odd particle, the heavy photon A_H cannot further decay into other particles, and would be a good candidate for the dark matter [23]. Since the CERN Large Hadron Collider (LHC) has potential to detect the signals of new gauge bosons and fermions, the phenomenology of the LHT would be quite interesting and a number of phenomenological works has been presented [20, 24, 25, 26].

In this paper, we present the QCD NLO corrections to the processes $pp \rightarrow W_H(Z_H)q_- + X$ [27] and $pp \rightarrow W_H^+ W_H^- + X$ [28].

2. The related LHT theory

Before our calculations, we will briefly recapitulate the LHT theory which is relevant to our work. The details of the LHT can be found in Refs.[18, 20, 21, 24].

At some high scale f the global symmetry $SU(5)$ is broken down to $SO(5)$, leading to 14 massless Nambu-Goldstone bosons. Four of them are manifested as the longitudinal modes of the heavy gauge bosons. The other 10 decompose into a T -even $SU(2)$ doublet h , identified as the SM Higgs field, and a complex T -odd $SU(2)$ triplet Φ , which obtains a mass of $m_\Phi = \sqrt{2}m_h f/v_{SM}$, with m_h and v_{SM} being SM Higgs mass and the electroweak symmetry break scale, respectively.

The additional discrete symmetry, T -parity, is in analogy to the R -parity in the minimal supersymmetric standard model (MSSM) [18, 20, 22]. The T -parity transformations for gauge sector are defined as the exchange between the gauge bosons of the two $SU(2) \times U(1)$ groups, i.e., $W_1^a \leftrightarrow W_2^a$ and $B_1 \leftrightarrow B_2$. Thus their T -odd and T -even combinations can be obtained as

$$\begin{aligned} W_H^a &= \frac{1}{\sqrt{2}}(W_1^a - W_2^a), & B_H &= \frac{1}{\sqrt{2}}(B_1 - B_2), & (T - odd), \\ W_L^a &= \frac{1}{\sqrt{2}}(W_1^a + W_2^a), & B_L &= \frac{1}{\sqrt{2}}(B_1 + B_2), & (T - even). \end{aligned} \quad (1)$$

The mass eigenstates of the gauge sector in the LHT are expressed as

$$\begin{aligned} W_H^\pm &= \frac{1}{\sqrt{2}}(W_H^1 \mp iW_H^2), & Z_H &= s_H B_H + c_H W_H^3, & A_H &= c_H B_H - s_H W_H^3, \\ W_L^\pm &= \frac{1}{\sqrt{2}}(W_L^1 \mp iW_L^2), & Z_L &= -s_w B_L + c_w W_L^3, & A_L &= c_w B_L + s_w W_L^3, \end{aligned} \quad (2)$$

where $s_w = \sin \theta_W$, $c_w = \cos \theta_W$, $s_H = \sin \theta_H$, $c_H = \cos \theta_H$, θ_W is the Weinberg angle, and the mixing angle θ_H at the $\mathcal{O}(v^2/f^2)$ is expressed as

$$\sin \theta_H \simeq \left[\frac{5gg'}{4(5g^2 - g'^2)} \frac{v_{SM}^2}{f^2} \right]. \quad (3)$$

Then the gauge sector consists of T -odd heavy new gauge bosons W_H^\pm , Z_H , A_H and T -even light gauge bosons identified as SM gauge bosons, W^\pm , Z^0 and one massless photon. The T parity partner of the photon, A_H , is the lightest T -odd particle, therefore, the candidate of dark matter in the LHT. The masses of the T parity partners of the photon, Z^0 - and W^\pm -boson are expressed as [24]

$$m_{W_H} \simeq m_{Z_H} \simeq gf \left(1 - \frac{1}{8} \frac{v_{SM}^2}{f^2} \right), \quad m_{A_H} \simeq \frac{1}{\sqrt{5}} g' f \left(1 - \frac{5}{8} \frac{v_{SM}^2}{f^2} \right), \quad (4)$$

where $v_{SM} = 246 \text{ GeV}$. At the tree level the SM gauge boson masses can be expressed as $m_W = \frac{gv_{SM}}{2}$ and $m_Z = \frac{v_{SM}\sqrt{g^2+g'^2}}{2}$.

In the LHT, the fermion sector of the first two generations in the SM is remained unchanged and the third generation of quarks is modified. We introduce two fermion doublets q_1 and q_2 for each fermion generation. The T parity transformation to these fermion doublets is defined as $q_1 \leftrightarrow -q_2$. Therefore, the T -odd and T -even combinations can be constructed as $q_- = \frac{1}{\sqrt{2}}(q_1 + q_2)$ and $q_+ = \frac{1}{\sqrt{2}}(q_1 - q_2)$, where q_+ is the doublet for the SM fermions and q_- for their T -odd partners. We take the Lagrangian suggested in Refs.[18, 20, 21] to generate the masses of the T -odd fermion doublets,

$$- \kappa f (\bar{\Psi}_2 \xi \Psi_c + \bar{\Psi}_1 \Sigma_0 \Omega \xi^\dagger \Omega \Psi_c) + \text{h.c.}, \quad (5)$$

where $\Omega = \text{diag}(1, 1, -1, 1, 1)$, $\Psi_c = (q_c, \chi_c, \tilde{q}_c)^T$, and the $SU(5)$ multiplets Ψ_1 and Ψ_2 are expressed as

$$\Psi_1 = \begin{pmatrix} q_1 \\ 0 \\ \mathbf{0}_2 \end{pmatrix}, \quad \Psi_2 = \begin{pmatrix} \mathbf{0}_2 \\ 0 \\ q_2 \end{pmatrix}. \quad (6)$$

The interaction Lagrangian in Eq.(5) can be proved to be invariant under T -parity, and T -odd quark doublet q_- gets a Dirac mass with $\tilde{q}_c \equiv (id_{R_-}, -iu_{R_-})^T$ from Eq.(5) expressed as [24]

$$m_{U_-} \simeq \sqrt{2} \kappa f \left(1 - \frac{1}{8} \frac{v_{SM}^2}{f^2} \right), \quad m_{D_-} = \sqrt{2} \kappa f, \quad (7)$$

where the lower indexes $U_- = u_-, c_-, t_-$ and $D_- = d_-, s_-, b_-$, which represent the T -odd heavy partners of the SM quarks, and κ is the mass coefficient in Lagrangian of the quark sector. As we know in the LHT $f > 500 \text{ GeV}$ [29], it is evident from Eq.(7) that the T -odd up- and down-type heavy partners have nearly equal masses.

In order to avoid the large radiative correction to Higgs boson mass induced by top-quark loop, the top sector must be additionally modified. We introduce the following two multiplets,

$$\mathcal{Q}_1 = \begin{pmatrix} q_1 \\ U_{L1} \\ \mathbf{0}_2 \end{pmatrix}, \quad \mathcal{Q}_2 = \begin{pmatrix} \mathbf{0}_2 \\ U_{L2} \\ q_2 \end{pmatrix}, \quad (8)$$

where U_{L1} and U_{L2} are the singlet fields and the q_1 and q_2 are the doublets. Under the $SU(5)$ and the T parity transformations, \mathcal{Q}_1 and \mathcal{Q}_2 behave themselves same as Ψ_1 and Ψ_2 .

In addition to the T -even SM top quark right-handed $SU(2)$ singlet u_R , the LHT contains two $SU(2)$ singlet fermions U_{R1} and U_{R2} of hypercharge $2/3$, which transform under T parity as

$$U_{R1} \leftrightarrow -U_{R2}. \quad (9)$$

The T parity invariant Yukawa Lagrangian of the top sector can be written as

$$\begin{aligned} \mathcal{L}_t^Y &= \frac{\lambda_1 f}{2\sqrt{2}} \epsilon_{ijk} \epsilon_{xy} [(\bar{Q}_1)_i \Sigma_{jx} \Sigma_{ky} - (\bar{Q}_2 \Sigma_0)_i \tilde{\Sigma}_{jx} \tilde{\Sigma}_{ky}] u_R \\ &+ \lambda_2 f (\bar{U}_{L1} U_{R1} + \bar{U}_{L2} U_{R2}) + \text{h.c.} . \end{aligned} \quad (10)$$

where $\tilde{\Sigma} = \Sigma_0 \Omega \Sigma^\dagger \Omega \Sigma_0$ is the image of the Σ field under T parity, and i, j and k run over 1 – 3 and x and y over 4 – 5. The T parity eigenstates are constructed as

$$q_\pm = \frac{1}{\sqrt{2}}(q_1 \mp q_2), \quad U_{L\pm} = \frac{1}{\sqrt{2}}(U_{L1} \mp U_{L2}), \quad U_{R\pm} = \frac{1}{\sqrt{2}}(U_{R1} \mp U_{R2}). \quad (11)$$

The T -odd states U_{L-} and U_{R-} combine to form a Dirac fermion T_- , and we obtain the mass of the T_- quark from the Lagrangian of Eq.(10) as

$$m_{T_-} = \lambda_2 f. \quad (12)$$

The left-handed (right-handed) top quark t is a linear combination of u_{L+} and U_{L+} (u_{R+} and U_{R+}), and another independent linear combination is a heavy T -even partner of the top quark T_+ :

$$\begin{pmatrix} t_X \\ T_{+X} \end{pmatrix} = \begin{pmatrix} c_X & -s_X \\ s_X & c_X \end{pmatrix} \begin{pmatrix} u_{X+} \\ U_{X+} \end{pmatrix}, \quad (X = L, R), \quad (13)$$

where the mixing matrix elements are approximately expressed as

$$s_L = s_\alpha^2 \frac{v_{SM}}{f} + \dots, \quad s_R = s_\alpha \left[1 - \frac{c_\alpha^2 (c_\alpha^2 - s_\alpha^2) v_{SM}^2}{2 f^2} + \dots \right]. \quad (14)$$

There we define $s_\alpha = \lambda_1 / \sqrt{\lambda_1^2 + \lambda_2^2}$ and $c_\alpha = \lambda_2 / \sqrt{\lambda_1^2 + \lambda_2^2}$. The t is identified with the SM top and T_+ is its T -even heavy partner. Then the masses of the top quark and T -even heavy top quark can be obtained as

$$m_t \simeq \frac{\lambda_1 \lambda_2 v_{SM}}{\sqrt{\lambda_1^2 + \lambda_2^2}}, \quad m_{T_+} \simeq f \sqrt{\lambda_1^2 + \lambda_2^2}. \quad (15)$$

The couplings of the T-odd $SU(2)$ doublet quarks and gauge bosons to the T-even SM particles used in our calculations are listed in Table 1 [20, 30], where $(V_{Hu})_{ij}$ and $(V_{Hd})_{ij}$ are the matrix elements of the CKM-like unitary mixing matrices V_{Hu} and V_{Hd} , respectively. The two mixing matrices satisfy $V_{Hu}^\dagger V_{Hd} = V_{CKM}$ [30], therefore, they cannot simultaneously be set to the identity. In the following calculations we take V_{Hu} to be a unit matrix, then we have $V_{Hd} = V_{CKM}$.

3. Renormalization and PROSPINO scheme

The strong coupling constant, the masses and wave functions of the relevant colored particles in the LHT are renormalized to remove the UV divergences of the virtual corrections. In our calculations, the following renormalization constants are introduced:

$$\begin{aligned} \psi_{q(q-)}^{0,L,R} &= \left(1 + \frac{1}{2} \delta Z_{q(q-)}^{L,R} \right) \psi_{q(q-)}^{L,R}, & m_{q-}^0 &= m_{q-} + \delta m_{q-}, \\ G_\mu^0 &= \left(1 + \frac{1}{2} \delta Z_g \right) G_\mu, & g_s^0 &= g_s + \delta g_s, \end{aligned} \quad (16)$$

Interaction	Feynman rule	Interaction	Feynman rule
$W_H^{+\mu} \bar{u}_-^i d_-^j$	$i \frac{g}{\sqrt{2}} (V_{Hd})_{ij} \gamma^\mu P_L$	$W_H^{-\mu} \bar{d}_-^i u_-^j$	$i \frac{g}{\sqrt{2}} (V_{Hu})_{ij} \gamma^\mu P_L$
$Z_H^\mu \bar{u}_-^i u_-^j$	$i \left(\frac{g C_H}{2} - \frac{g' S_H}{10} \right) (V_{Hu})_{ij} \gamma^\mu P_L$	$Z_H^\mu \bar{d}_-^i d_-^j$	$i \left(-\frac{g C_H}{2} - \frac{g' S_H}{10} \right) (V_{Hd})_{ij} \gamma^\mu P_L$
$\bar{q}_-^\alpha q_-^\beta G_\mu^a$	$i g_s (T^a)_{\alpha\beta} \gamma^\mu$		

Table 1. The related LHT Feynman rules used in our calculations, where $q_- = u_-, d_-, c_-, s_-, t_-, b_-$, i and j are the generation indices and $C_H^2 = 1 - S_H^2$.

where g_s denotes the strong coupling constant, m_{q_-} is the T-odd quark mass, $\psi_{q(q_-)}^{L,R}$ and G_μ denote the fields of the SM quark, T-odd heavy quark and gluon, respectively. The masses and wave functions of the colored fields are renormalized by adopting the on-shell scheme, then the relevant renormalization constants are expressed as

$$\delta Z_q^{L,R} \equiv \delta Z_q = -\frac{\alpha_s(\mu_r)}{3\pi} \left[\Delta_{UV} - \Delta_{IR} \right], \quad (17)$$

$$\delta Z_{q_-}^{L,R} \equiv \delta Z_{q_-} = -\frac{\alpha_s(\mu_r)}{3\pi} \left[\Delta_{UV} + 2\Delta_{IR} + 4 + 3 \ln \left(\frac{\mu_r^2}{m_{q_-}^2} \right) \right], \quad (18)$$

$$\frac{\delta m_{q_-}}{m_{q_-}} = -\frac{\alpha_s(\mu_r)}{3\pi} \left\{ 3 \left[\Delta_{UV} + \ln \left(\frac{\mu_r^2}{m_{q_-}^2} \right) \right] + 4 \right\}, \quad (19)$$

$$\delta Z_g = -\frac{\alpha_s(\mu_r)}{2\pi} \left\{ \frac{3}{2} \Delta_{UV} + \frac{5}{6} \Delta_{IR} + \frac{1}{3} \ln \left(\frac{\mu_r^2}{m_t^2} \right) + \frac{1}{3} \sum_{T=T_+}^{T_-} \ln \left(\frac{\mu_r^2}{m_T^2} \right) + \frac{1}{3} \sum_{q_-} \ln \frac{\mu_r^2}{m_{q_-}^2} \right\}, \quad (20)$$

$(q_- = u_-, d_-, c_-, s_-, t_-, b_-)$,

where $\Delta_{UV} = 1/\epsilon_{UV} - \gamma_E + \ln(4\pi)$ and $\Delta_{IR} = 1/\epsilon_{IR} - \gamma_E + \ln(4\pi)$.

For the renormalization of the strong coupling constant g_s , we adopt the \overline{MS} scheme at the renormalization scale μ_r , except that the divergences associated with the massive top-quark, T-odd $SU(2)$ doublet quarks ($u_-, d_-, c_-, s_-, t_-, b_-$) and T_\pm loops are subtracted at zero momentum [31]. Then the renormalization constant of the strong coupling constant can be obtained as

$$\frac{\delta g_s}{g_s} = -\frac{\alpha_s(\mu_r)}{4\pi} \left[\frac{3}{2} \Delta_{UV} + \frac{1}{3} \ln \frac{m_t^2}{\mu_r^2} + \frac{1}{3} \sum_{T=T_+}^{T_-} \ln \frac{m_T^2}{\mu_r^2} + \frac{1}{3} \sum_{q_-} \ln \frac{m_{q_-}^2}{\mu_r^2} \right], \quad (21)$$

$(q_- = u_-, d_-, c_-, s_-, t_-, b_-)$.

In the calculation, we can find there are additional on-shell T-odd quark resonance in the real light-quark emissions. We adopt the PROSPINO scheme [32, 33] to remove them. The PROSPINO scheme is defined as a replacement of the Breit-Wigner propagator [33]

$$\frac{|\mathcal{M}|^2(s_{V_H q})}{(s_{V_H q} - m_{q_-}^2)^2 + m_{q_-}^2 \Gamma_{q_-}^2} \rightarrow \frac{|\mathcal{M}|^2(s_{V_H q})}{(s_{V_H q} - m_{q_-}^2)^2 + m_{q_-}^2 \Gamma_{q_-}^2} - \frac{|\mathcal{M}|^2(m_{q_-}^2)}{(s_{V_H q} - m_{q_-}^2)^2 + m_{q_-}^2 \Gamma_{q_-}^2} \Theta(\hat{s} - 4m_{q_-}^2) \Theta(m_{q_-} - m_{V_H}), \quad (22)$$

where $s_{V_H q}$ is the squared momentum flowing through the intermediate q_- propagator.

4. Numerical results of $pp \rightarrow W_H(Z_H)q_- + X$ process

Due to the additional T-odd quark resonance in light-quark emission subprocesses, we apply three schemes in considering the QCD NLO corrections in this work. In scheme (I) (denoted as ‘‘QCD NLO I’’) we include all light-quark emission contributions in the QCD NLO corrections. In scheme (II) (denoted as ‘‘QCD NLO II’’) we exclude the contributions of the partonic processes of light-quark emission. The PROSPINO scheme for light-quark emission is used in scheme (III).

In the study of the dependence of the QCD NLO corrected cross section on the factorization and renormalization scales, we set the two unphysical scales equal to a common value ($\mu_f = \mu_r = \mu$) and do not vary them in an independent way for simplicity.

We take one-loop and two-loop running α_s in the LO and QCD NLO calculations, respectively [34]. The central value of the factorization/renormalization scale μ is chosen as $\mu_0 = (m_{W_H} + m_{d_-})/2$. We adopt the CTEQ6L1 and CTEQ6M parton densities with five flavors in the LO and NLO calculations, respectively [35]. The strong coupling constant $\alpha_s(\mu)$ is determined by the QCD parameter $\Lambda_5^{LO} = 165 \text{ MeV}$ for the CTEQ6L1 at the LO and $\Lambda_5^{\overline{MS}} = 226 \text{ MeV}$ for the CTEQ6M at the NLO [34]. We ignore the masses of u -, d -, c -, s -, b -quarks, and take $\alpha_{ew}(m_Z^2)^{-1}|_{\overline{MS}} = 127.925$, $m_W = 80.399 \text{ GeV}$, $m_Z = 91.1876 \text{ GeV}$, $m_t = 171.2 \text{ GeV}$ and $\sin^2 \theta_W = 1 - \left(\frac{m_W}{m_Z}\right)^2 = 0.222646$.

The colliding energy in the proton-proton center-of-mass system is taken as $\sqrt{s} = 7 \text{ TeV}$ for the early LHC and $\sqrt{s} = 14 \text{ TeV}$ for the later running at the LHC. The Cabibbo-Kobayashi-Maskawa (CKM) matrix elements are taken as

$$V_{CKM} = \begin{pmatrix} V_{ud} & V_{us} & V_{ub} \\ V_{cd} & V_{cs} & V_{cb} \\ V_{td} & V_{ts} & V_{tb} \end{pmatrix} = \begin{pmatrix} 0.97418 & 0.22577 & 0 \\ -0.22577 & 0.97418 & 0 \\ 0 & 0 & 1 \end{pmatrix}. \quad (23)$$

4.1. Dependence on factorization/renormalization scale

In Figs.1(a,b,c) and Figs.2(a,b,c) we present the LO, QCD NLO corrected cross sections and the corresponding K-factors for the $pp \rightarrow W_H q_- + X$ and $pp \rightarrow Z_H q_- + X$ processes as the functions of the factorization/renormalization scale at the LHC with $\sqrt{s} = 7 \text{ TeV}$ and 14 TeV , respectively. In Figs.1(a,b) and Figs.2(a,b) the LHT input parameters are taken as $f = 500 \text{ GeV}$ and $\kappa = 1$, while in Fig.1(c) and Fig.2(c) we take $f = 1 \text{ TeV}$ and $\kappa = 1$. In these figures the curves labeled by ‘‘NLO I’’, ‘‘NLO II’’ and ‘‘NLO III’’ are for the QCD NLO corrected cross sections using the (I), (II) and (III) schemes, respectively. The figures show that by using the (II) and (III) subtraction schemes we can get almost the same and moderate QCD NLO corrections to the production rate with a strongly reduced factorization/renormalization scale uncertainty in the plotted range of μ , while the QCD NLO corrections using the scheme (I) do not obviously improve the scale dependence of the LO cross section and destroy the perturbative convergence in some range of μ . In the following analysis we set the factorization/renormalization scale μ as its central value $\mu_0 = (m_{W_H} + m_{d_-})/2$.

4.2. Dependence on LHT parameters

We depict the LO, QCD NLO corrected cross sections and the corresponding K-factors for the $pp \rightarrow W_H q_- + X$ and $pp \rightarrow Z_H q_- + X$ processes as the functions of f , the $SU(5)$ global symmetry breaking scale of the LHT, at the LHC with $\sqrt{s} = 7 \text{ TeV}$ and 14 TeV in Figs.3(a,b,c) and Figs.4(a,b,c), respectively. In Figs.3(a,b) and Figs.4(a,b) the parameter κ is set to be 1, while in Fig.3(c) and Fig.4(c) we take $\kappa = 3$. The curves labeled by ‘‘NLO I’’, ‘‘NLO II’’ and ‘‘NLO III’’ are for the QCD NLO corrected cross sections using the (I), (II) and (III) schemes, respectively. One can conclude from these figures that the cross section for the $pp \rightarrow W_H(Z_H)q_- + X$ process decreases quickly with the increment of f , because the two final T-odd particles become heavier

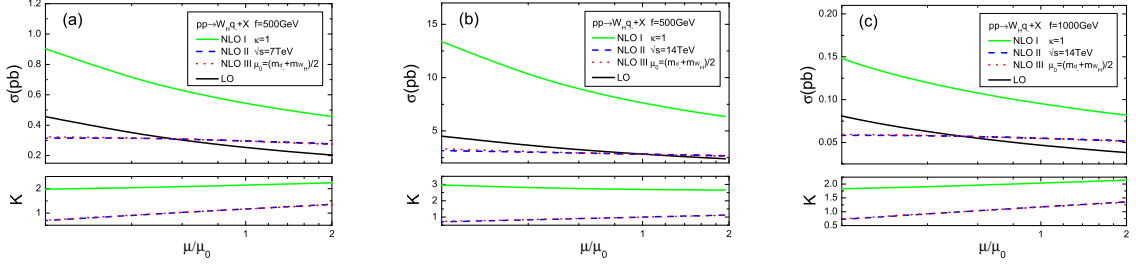


Figure 1. The dependence of the cross sections and the corresponding K-factors for the $pp \rightarrow W_H q_- + X$ process on the factorization/renormalization scale μ at the LHC. (a) $f = 500 \text{ GeV}$, $\kappa = 1$ and $\sqrt{s} = 7 \text{ TeV}$. (b) $f = 500 \text{ GeV}$, $\kappa = 1$ and $\sqrt{s} = 14 \text{ TeV}$. (c) $f = 1 \text{ TeV}$, $\kappa = 1$ and $\sqrt{s} = 14 \text{ TeV}$.

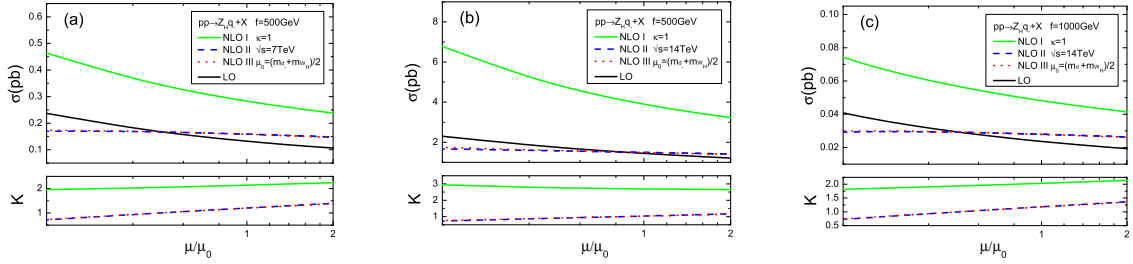


Figure 2. The dependence of the cross sections and the corresponding K-factors for the $pp \rightarrow Z_H q_- + X$ process on the factorization/renormalization scale μ at the LHC. (a) $f = 500 \text{ GeV}$, $\kappa = 1$ and $\sqrt{s} = 7 \text{ TeV}$. (b) $f = 500 \text{ GeV}$, $\kappa = 1$ and $\sqrt{s} = 14 \text{ TeV}$. (c) $f = 1 \text{ TeV}$, $\kappa = 1$ and $\sqrt{s} = 14 \text{ TeV}$.

with the increment of f . However, in the plotted range of f we could have observable production rates for the $pp \rightarrow W_H q_- + X$ and $pp \rightarrow Z_H q_- + X$ processes, especially when $\kappa = 1$.

5. Numerical results of $pp \rightarrow W_H^+ W_H^- + X$ process

We take $\alpha_{ew}(m_Z^2)^{-1} = 127.916$, $m_W = 80.399 \text{ GeV}$, $m_Z = 91.1876 \text{ GeV}$, $\sin^2 \theta_W = 1 - \left(\frac{m_W}{m_Z}\right)^2 = 0.2226$ and $m_t = 171.2 \text{ GeV}$ [34]. The masses of all the SM leptons and quarks except top quark are neglected. The center-of-mass energies \sqrt{s} of proton-proton collision are taken to be 14 TeV and 8 TeV for the future and early LHC, separately. We set the factorization and renormalization scale to be equal ($\mu_r = \mu_f$) and define $\mu_0 = m_{W_H}$. We employ CTEQ6L1 and CTEQ6M in the the LO and NLO calculations respectively [35], and fix the LHT parameters $\kappa = 1$ and $s_\alpha = c_\alpha = \frac{\sqrt{2}}{2}$. In this work we only use the PROSPINO scheme to deal with the real-quark emission subprocesses.

5.1. Dependence on factorization/renormalization scale

In Figs.5(a,b) we present the dependence of the LO, QCD NLO corrected integrated cross sections and the corresponding K-factor ($K \equiv \sigma_{NLO}/\sigma_{LO}$) on the factorization/renormalization

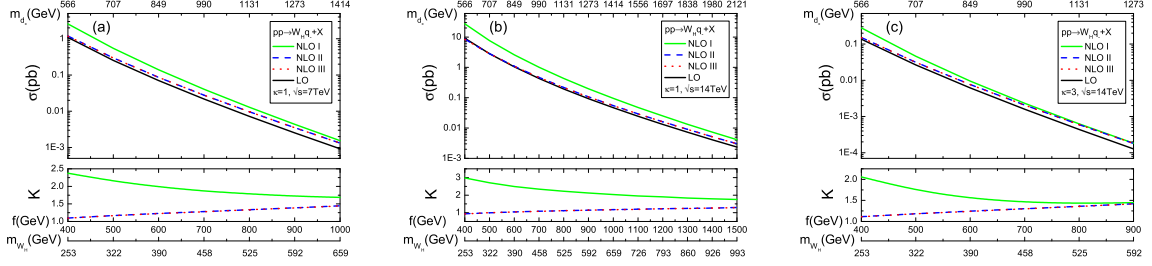


Figure 3. The cross sections and the corresponding K -factors for the $pp \rightarrow W_H q_- + X$ process as the functions of the LHT parameter f at the LHC. The corresponding m_{W_H} and m_{d_-} values are also scaled on the x-axis. (a) $\kappa = 1$ and $\sqrt{s} = 7 \text{ TeV}$. (b) $\kappa = 1$ and $\sqrt{s} = 14 \text{ TeV}$. (c) $\kappa = 3$ and $\sqrt{s} = 14 \text{ TeV}$.

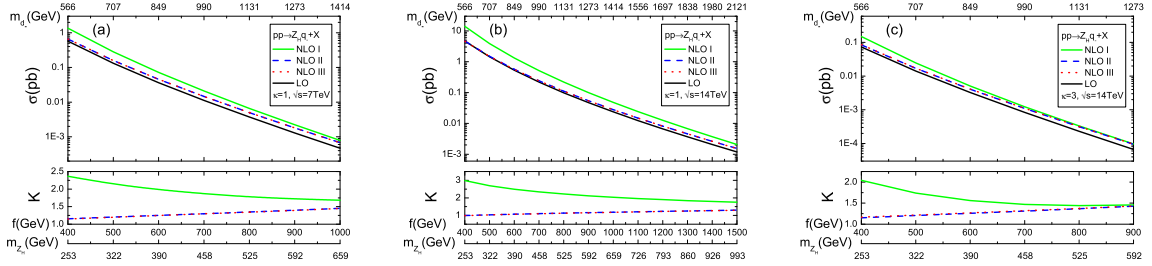


Figure 4. The cross sections and the corresponding K -factors for the $pp \rightarrow Z_H q_- + X$ process as the functions of the LHT parameter f at the LHC. The corresponding m_{W_H} and m_{d_-} values are also scaled on the x-axis. (a) $\kappa = 1$ and $\sqrt{s} = 7 \text{ TeV}$. (b) $\kappa = 1$ and $\sqrt{s} = 14 \text{ TeV}$. (c) $\kappa = 3$ and $\sqrt{s} = 14 \text{ TeV}$.

scale μ for the process $pp \rightarrow W_H^+ W_H^- + X$ at the $\sqrt{s} = 14 \text{ TeV}$ and the $\sqrt{s} = 8 \text{ TeV}$ LHC separately, where we take the LHT parameters $f = 800 \text{ GeV}$, $\kappa = 1$ and $s_\alpha = c_\alpha = \frac{\sqrt{2}}{2}$. From the curves in Figs.5(a,b), we find that QCD NLO corrections to the $pp \rightarrow W_H^+ W_H^- + X$ process significantly reduce the scale uncertainty. We can read out from the figures that the LO and QCD NLO corrected cross sections at $\mu_0 = m_{W_H}$ are $\sigma_{LO}(\sqrt{s} = 14 \text{ TeV}) = 32.63^{+9.56}_{-6.38} \text{ fb}$, $\sigma_{NLO}(\sqrt{s} = 14 \text{ TeV}) = 37.43^{+2.19}_{-2.83} \text{ fb}$ and $\sigma_{LO}(\sqrt{s} = 8 \text{ TeV}) = 5.54^{+2.71}_{-1.51} \text{ fb}$, $\sigma_{NLO}(\sqrt{s} = 8 \text{ TeV}) = 6.14^{+0.26}_{-0.70} \text{ fb}$, where the uncertainties describe the missing higher-order corrections estimated via scale variations in the range of $0.1\mu_0 < \mu < 10\mu_0$. The K -factor varies from 0.94 (0.77) to 1.32 (1.35) at the $\sqrt{s} = 14 \text{ TeV}$ (8 TeV) LHC, when μ/μ_0 goes from 0.1 to 10. With the definition of scale uncertainty as $\eta = \frac{|\sigma(0.1\mu_0) - \sigma(10\mu_0)|}{\sigma(\mu_0)}$, we obtain that the scale uncertainties are reduced from 48.88% (LO) to 13.40% (NLO) at the $\sqrt{s} = 14 \text{ TeV}$ and from 76.23% (LO) to 14.54% (NLO) at the $\sqrt{s} = 8 \text{ TeV}$ LHC, respectively. In Table 2 we list some numerical results of the cross sections and K -factors for some typical values of μ/μ_0 , which are read out from Figs.5(a,b). In order to investigate the contribution from the $pp \rightarrow gg \rightarrow W_H^+ W_H^- + X$ process, which is considered as a component of the QCD NLO corrections to the parent process $pp \rightarrow W_H^+ W_H^- + X$, we also present the cross sections for the $pp \rightarrow gg \rightarrow W_H^+ W_H^- + X$ process ($\sigma(gg)$) in this table. We can obtain from the data that the QCD NLO correction part from

\sqrt{s} (TeV)	μ/μ_0	σ_{LO} (fb)	σ_{NLO} (fb)	$\sigma(gg)$ (fb)	K
14	0.1	42.190(1)	39.62(2)	0.993(1)	0.939
	0.5	35.091(1)	38.17(2)	0.3946(6)	1.09
	1	32.626(1)	37.43(2)	0.2810(5)	1.15
	2	30.444(1)	37.53(2)	0.2056(4)	1.20
	10	26.242(1)	34.60(2)	0.1081(2)	1.32
8	0.1	8.2548(4)	6.333(3)	0.0805(1)	0.767
	0.5	6.1850(3)	6.300(3)	0.02842(3)	1.019
	1	5.5417(2)	6.143(3)	0.01943(3)	1.11
	2	5.0006(2)	5.947(3)	0.01371(2)	1.21
	10	4.0304(2)	5.440(2)	0.00671(1)	1.40

Table 2. The numerical results of σ_{LO} , σ_{NLO} and the corresponding K -factors at the 14 TeV and the 8 TeV LHC by taking $f = 800$ GeV, $\kappa = 1$, $s_\alpha = c_\alpha = \frac{\sqrt{2}}{2}$ and some typical values of factorization/renormalization scale μ . $\sigma(gg)$ is the cross section for the $pp \rightarrow gg \rightarrow W_H^+ W_H^- + X$ process, which is considered as a component of the QCD NLO correction to the parent process $pp \rightarrow W_H^+ W_H^- + X$.

the $pp \rightarrow gg \rightarrow W_H^+ W_H^- + X$ process at $\mu = \mu_0$ is about 5.85% (3.23%) of the total QCD NLO correction ($\Delta\sigma_{NLO}$) at the 14 TeV (8 TeV) LHC. We can see also that the NLO theoretical uncertainty due the choice of μ mainly comes from the genuine QCD NLO corrected cross section for the $pp \rightarrow q\bar{q} \rightarrow W_H^+ W_H^- + X$ process, while the contribution from the $pp \rightarrow gg \rightarrow W_H^+ W_H^- + X$ process is relatively small. In further numerical calculations we fix the renormalization and factorization scales being equal to their central value, i.e., $\mu = \mu_r = \mu_f = \mu_0 = m_{W_H}$.

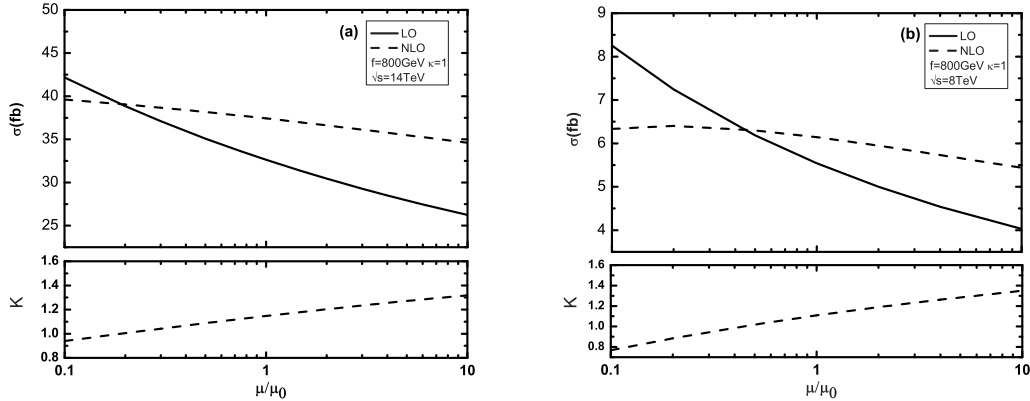


Figure 5. The dependence of the LO, QCD NLO corrected integrated cross sections and the corresponding K -factors for the $pp \rightarrow W_H^+ W_H^- + X$ process on the factorization/renormalization scale μ at the LHC with $f = 800$ GeV, $\kappa = 1$ and $s_\alpha = c_\alpha = \frac{\sqrt{2}}{2}$. (a) $\sqrt{s} = 14$ TeV. (b) $\sqrt{s} = 8$ TeV.

5.2. Dependence on global symmetry breaking scale f

The LO and QCD NLO corrected integrated cross sections together with the corresponding K -factor as functions of the scale f at the $\sqrt{s} = 14 \text{ TeV}$ and the $\sqrt{s} = 8 \text{ TeV}$ LHC are depicted in Figs.6(a) and (b), respectively. We can see from Fig.6 that the LO and NLO total cross sections for the $pp \rightarrow W_H^+ W_H^- + X$ process decrease drastically when f goes up. This is because the mass of final W_H becomes heavier as the increment of f , therefore the phase-space becomes smaller. We can read out from the figures that the corresponding K -factor varies from 1.22 to 1.10 at the $\sqrt{s} = 14 \text{ TeV}$ LHC and from 1.17 to 1.10 at the $\sqrt{s} = 8 \text{ TeV}$ LHC in the plotted f range. In Table 3, we list some numerical results of the LO, NLO cross sections and the corresponding K -factors for some typical values of f which are shown in Figs.6(a,b).

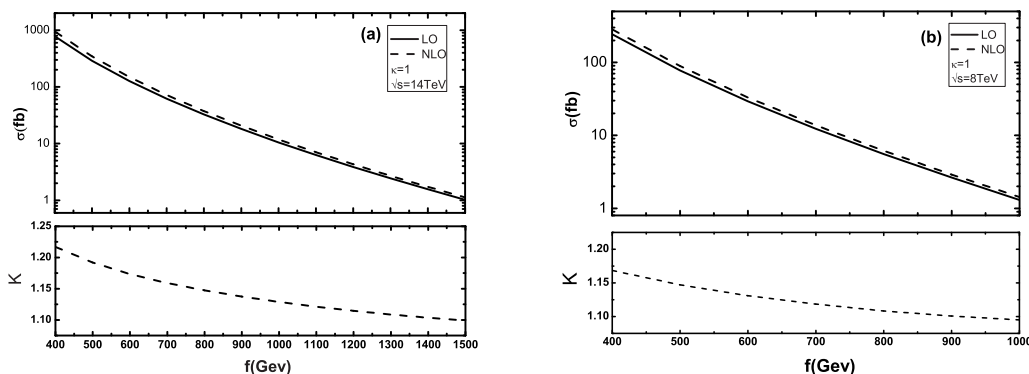


Figure 6. The LO, QCD NLO corrected integrated cross sections and the corresponding K -factors for the $pp \rightarrow W_H^+ W_H^- + X$ process as the functions of the global symmetry breaking scale f at the LHC with $\kappa = 1$ and $s_\alpha = c_\alpha = \frac{\sqrt{2}}{2}$. (a) $\sqrt{s} = 14 \text{ TeV}$. (b) $\sqrt{s} = 8 \text{ TeV}$.

6. Summary

In this paper, we present the calculation of $W_H(Z_H)q_-$ and W_H -pair productions at the $\sqrt{s} = 14 \text{ TeV}$ and the $\sqrt{s} = 8 \text{ TeV}$ LHC in QCD NLO. The dependence of the total cross section on the renormalization/factorization scale shows that the QCD NLO corrections can reduce significantly the uncertainty of the LO theoretical predictions. We also display the dependence of cross sections on global symmetry breaking scale f . The more calculation detail and numerical results were presented in Refs.[27, 28].

Acknowledgments: This work was supported in part by the National Natural Science Foundation of China (Contract No.11075150, No.11005101), and the Specialized Research Fund for the Doctoral Program of Higher Education (Contract No.20093402110030).

- [1] S. L. Glashow, Nucl. Phys. **22** (1961) 579; S. Weinberg, Phys. Rev. Lett. **19** (1967) 1264; A. Salam, Proc. 8th Nobel Symposium Stockholm 1968, ed. N. Svartholm (Almqvist and Wiksells, Stockholm 1968) p.367; H. D. Politzer, Phys. Rept. **14** (1974) 129.
- [2] P. W. Higgs, Phys. Lett. **12** (1964) 132, Phys. Rev. Lett. **13** (1964) 508, Phys. Rev. **145** (1966) 1156; F. Englert and R. Brout, Phys. Rev. Lett. **13** (1964) 321; G. S. Guralnik, C. R. Hagen and T. W. B. Kibble, Phys. Rev. Lett. **13** (1964) 585; T. W. B. Kibble, Phys. Rev. **155** (1967) 1554.

\sqrt{s} (<i>TeV</i>)	f (<i>GeV</i>)	σ_{LO} (<i>fb</i>)	σ_{NLO} (<i>fb</i>)	K
14	500	289.93(1)	345.6(2)	1.19
	700	62.053(3)	71.93(4)	1.16
	800	32.626(1)	37.43(2)	1.15
	900	18.1252(8)	20.61(1)	1.14
	1100	6.2964(3)	7.059(3)	1.12
	1300	2.44312(9)	2.709(1)	1.11
	1500	1.02314(4)	1.1246(5)	1.10
8	500	77.693(3)	89.12(5)	1.15
	700	12.2863(5)	13.741(7)	1.12
	800	5.5417(2)	6.143(3)	1.11
	900	2.6357(1)	2.901(1)	1.10

Table 3. The numerical results of σ_{LO} , σ_{NLO} and the corresponding K -factors at the $\sqrt{s} = 14$ *TeV* and the $\sqrt{s} = 8$ *TeV* LHC by taking $\kappa = 1$, $s_\alpha = c_\alpha = \frac{\sqrt{2}}{2}$, $\mu = \mu_0$ and some typical values of f .

- [3] G.G. Ross, Grand Unied Theories (Addison-Wesley Publishing Company, Reading, MA, (1984); P. Langacker, Phys. Rep. 72 (1981) 185; H. Georgi, S.L. Glashow, Phys. Rev. Lett. 32 (1974) 438; A.J. Buras, J. Ellis, M.K. Gaillard, D.V. Nanopoulos, Nucl. Phys. **B135**(1978) 66.
- [4] S. P. Martin, arXiv:hep-ph/9709356; M. E. Peskin, arXiv:0801.1928 [hep-ph]; K. A. Olive, arXiv:hep-ph/9911307; M. Drees, arXiv:hep-ph/9611409; H. E. Haber and G. L. Kane, Phys. Rept. 117 (1985) 75; H. P. Nilles, Phys. Rept. 110, 1 (1984); A. Signer, J.Phys.**G36** (2009) 073002, arXiv:0905.4630 [hep-ph].
- [5] N. Arkani-Hamed, S. Dimopoulos, G. Dvali, Phys. Lett. B429 (34): 263(1998), arXiv:hep-ph/9803315; N. Arkani-Hamed, S. Dimopoulos, G. Dvali, Phys. Rev. D59 086004(1999), arXiv:hep-ph/9807344; I. Antoniadis, N. Arkani-Hamed, S. Dimopoulos, G. Dvali, Phys. Lett. **B436** (34): 257(1998), arXiv:hep-ph/9804398; M. Shifman, Int. J. Mod. Phys. **A25** 199-225,2010, arXiv:0907.3074v2 [hep-ph].
- [6] R. N. Mohapatra and J. C. Pati, Phys. Rev. **D11** (1975), 566571; G. Senjanovic and R. N. Mohapatra; Phys. Rev. **D12** (1975), 1502; A. Adulpravitchai, M. Lindner, A. Merle, and R. N. Mohapatra, Phys. Lett. **B680** (2009) 476, arXiv/hep-ph:0908.0470.
- [7] L.Basso, S. Moretti, G.M. Pruna, Phys. Rev.**D83**(2011) 055014, arXiv:1011.2612v4 [hep-ph].
- [8] N. Arkani-Hamed, A. G. Cohen and H. Georgi, Phys. Lett. **B513** (2001) 232; M. Schmaltz and D. Tucker-Smith, Ann. Rev. Nucl. Part. Sci. **55** (2005) 229; M. Perelstein, Prog. Part. Nucl. Phys. **58** (2007) 247; and references therein.
- [9] Arkani-Hamed, A. G. Cohen, E. Katz, A. E. Nelson, T. Gregoire and J. G. Wacker, JHEP **08** (2002) 021.
- [10] N. Arkani-Hamed, A. G. Cohen, T. Gregoire, J. G. Wacker and A. G. Cohen, JHEP **08** (2002) 020.
- [11] I. Low, W. Skiba and D.Smith, Phys. Rev. **D66**, (2002) 072001.
- [12] C. Csaki, J. Hubisz, G. D. Kribs, P. Meade and J. Terning, Phys. Rev. **D67** (2003) 115002, [arXiv:hep-ph/0211124].
- [13] M. Schmaltz, Nucl. Phys. Proc. Suppl. **117** (2003) 40.
- [14] T. Gregoire and J. G. Wacker, JHEP **08** (2002) 019.
- [15] N. Arkani-Hamed, A. G. Cohen, E. Katz and A. E. Nelson, JHEP **07** (2002) 034.
- [16] ATLAS Collaboration, Phys. Lett. **B705** (2011) 18-46.
- [17] D. Olivito, for the ATLAS collaboration, Conference proceedings for the Meeting of the Division of Particles and Fields of the American Physical Society (DPF), 2011, arXiv:1109.0934.
- [18] I. Low, JHEP **0410** (2004) 067.
- [19] R. Barbieri and A. Strumia, IFUP-TH/2000-22 and SNS-PH/00-12, [arXiv:hep-ph/0007265].
- [20] J. Hubisz and P. Meade, Phys. Rev. **D71** (2005) 035016.
- [21] J. Hubisz, P. Meade, A. Noble and M. Perelstein, JHEP **01** (2006) 135.
- [22] H.-C. Cheng and I. Low, **JHEP** 09 (2003) 051; **JHEP** 08 (2004) 061.
- [23] A. Birkedal, A. Noble, M. Perelstein and A. Spray, Phys. Rev. **D74** (2006) 035002; M. Asano, S. Matsumoto,

- N. Okada, and Y. Okada, Phys. Rev. **D75** (2007) 063506.
- [24] A. Belyaev, C. -R. Chen, K. Tobe and C. -P. Yuan, Phys. Rev. **D74**, (2006) 115020.
- [25] A. Belyaev, C. -R. Chen, K. Tobe and C. -P. Yuan, in Proceedings of Monte Carlo Tools for Beyond the Standard Model Physics, Fermilab, 2006, given by A. Belyaev, <http://theory.fnal.gov/mc4bsm/agenda.html>; in Proceedings of Osaka University, 2006, Osaka, given by C. -P. Yuan, <http://www-het.phys.sci.osaka-u.ac.jp/seminar/seminar/seminar.html>; in Proceedings of the Summer Institute on Collider Phenomenology, National Tsing Hua University, Taiwan, 2006, given by K. Tobe, <http://charm.phys.nthu.edu.tw/hep/summer2006/>; in Proceedings of ICHEP'06, Moscow, 2006, given by A. Belyaev, http://ichep06.jinr.ru/reports/116_11s1_10p20_belyaev.pdf.
- [26] C.-S. Chen, K. Cheung and T. -C. Yuan, Phys. Lett. **B644** (2007) 158.
- [27] R.-Y. Zhang, H. Yan, W.-G. Ma, S.-M. Wang, L. Guo and L. Han, Phys. Rev. **D85** (2012)015017.
- [28] S.-M. Du, L. Guo, W. Liu, W.-G. Ma and R.-Y. Zhang, Phys. Rev. **D86** (2013) 054027.
- [29] J. Hubisz, P. Meade, A. Noble and M. Perelstein, JHEP **0601**, 135 (2006), arXiv:hep-ph/0506042.
- [30] M. Blanke, A. J. Buras, A. Poschenrieder, S. Recksiegel, C. Tarantino, S. Uhlig and A. Weiler JHEP **01** (2007) 066.
- [31] J. Collins, F. Wilczek, and A. Zee, Phys. Rev. **D18** (1978) 242; W. J. Marciano, Phys. Rev. **D29** (1984) 580; P. Nason, S. Dawson and R.K. Ellis, Nucl. Phys. **B327** (1989) 49, Nucl. Phys. **B335** (1990) 260(E).
- [32] W. Beenakker, R. Höpker, M. Spira and P. M. Zerwas, Nucl. Phys. **B492** (1997) 51; W. Beenakker, M. Klasen, M. Krämer, T. Plehn, M. Spira and P. M. Zerwas, Phys. Rev. Lett. **83** (1999) 3780; <http://www.thphys.uni-heidelberg.de/~plehn/index.php?show=prospino>.
- [33] T. Plehn and C. Weydert, PoS **CHARGED2010** (2010) 026, [arXiv:1012.3761]; T. Binoth, D. Goncalves-Netto, D. Lopez-Val, K. Mawatari, T. Plehn and I. Wigmore, Phys. Rev. D **84** (2011) 075005, [arXiv:1108.1250].
- [34] K. Nakamura, *et al.*, J. Phys. **G37** (2010) 075021.
- [35] J. Pumplin, D. R. Stump, J. Huston, H. -L. Lai, P. Nadolsky and W. -K. Tung, JHEP **07** (2002) 012; D. Stump, J. Huston, J. Pumplin, W. -K. Tung, H. -L. Lai, S. Kuhlmann and J. F. Owens, JHEP **10** (2003) 046.